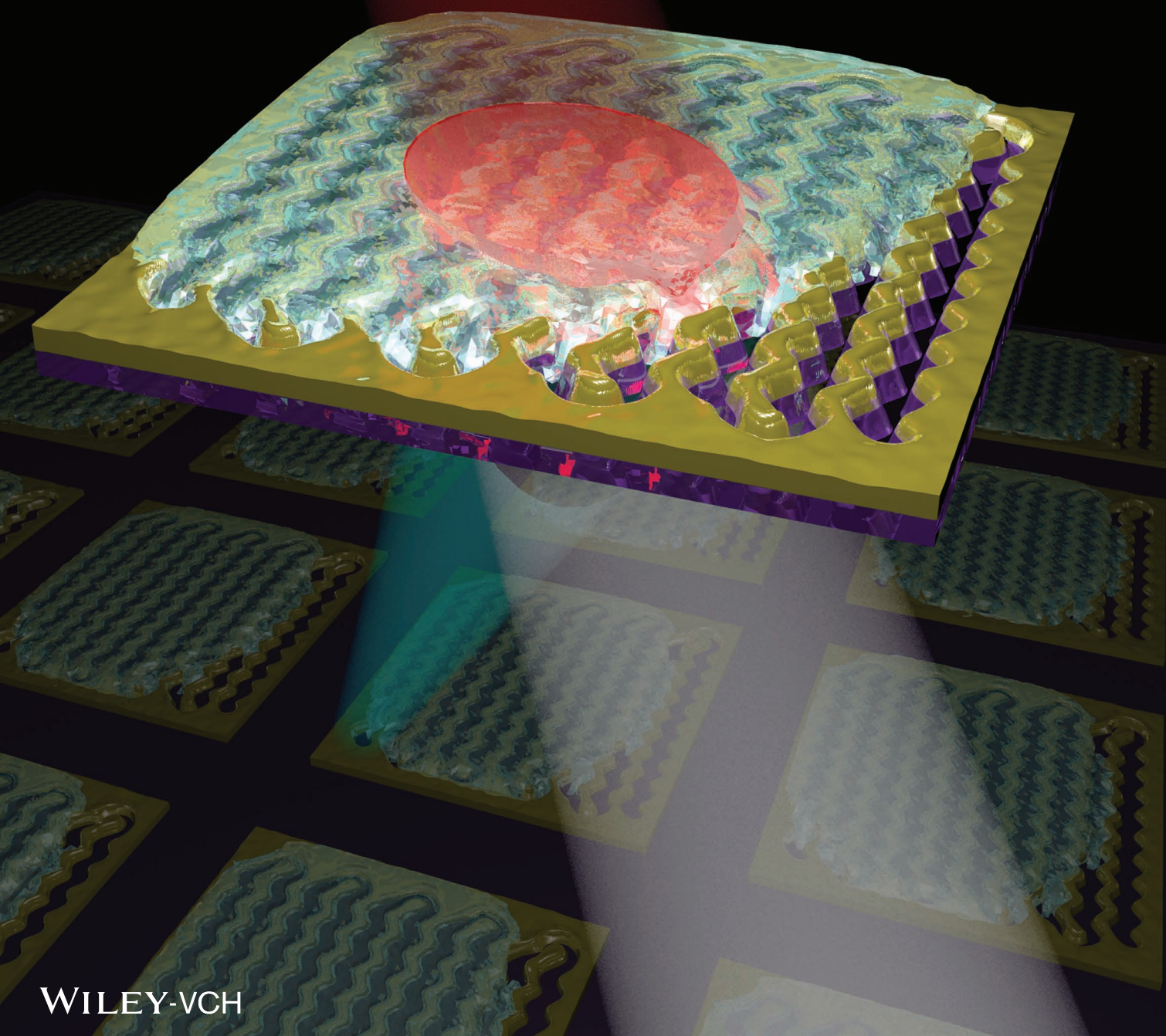


ADVANCED OPTICAL MATERIALS



Electrically Controlled Nanostructured Metasurface Loaded with Liquid Crystal: Toward Multifunctional Photonic Switch

Oleksandr Buchnev,* Nina Podoliak, Malgosia Kaczmarek, Nikolay I. Zheludev, and Vassili A. Fedotov*

Achieving an efficient spectral tuning in liquid-crystal (LC)-loaded active photonic metamaterials has so far remained a challenge due to strong surface anchoring of LC molecules. This paper reports on a novel approach in the development of hybrid metamaterials that enables to overcome this problem and engage for the first time in-plane switching of liquid-crystal molecules on the nanoscale. Combined with the usual volume switching, it unlocks the full potential of the liquid crystals as a functional component of active metamaterial hybrids operating at optical frequencies. As a result, the resonant response of an active metasurface can now be controlled both in terms of its magnitude and wavelength with the spectral tunability approaching the theoretical limit of 9%. This mechanism of two-way active switching of the hybrid metamaterial is also confirmed theoretically by simulating the distribution of the LC director around the metamaterial fabric.

and absorb light with no diffraction. Planar metamaterials offer unprecedented flexibility in the design and control of light propagation, replacing bulk optical components,^[1–5] and exhibiting exotic optical effects, such as asymmetric transmission^[6] and extrinsic optical activity,^[7] whereas recent demonstrations of anomalous reflection and refraction by metasurfaces have opened a new exciting chapter in photonic research.^[8,9] Metasurfaces can be readily fabricated using existing planar technologies, while hybridization of their fabric with naturally available functional materials should enable dynamic control over their optical properties, dramatically expanding the range of potential metamaterial applications.^[10,11]

1. Introduction

Metasurfaces (or planar metamaterials) represent a special class of low-dimensional artificial photonic media—periodically structured metallic surfaces and thin films that can transmit, reflect,

and among the existing functional materials, liquid crystals (LCs) possess arguably the strongest and most broadband optical non-linearity and birefringence, which can be externally controlled by temperature, light, and electric or magnetic fields.^[12] That has made liquid crystals, and nematics in particular, one of the first and most popular active ingredients considered for hybrid metamaterial and plasmonic designs.^[13–21] Although the refractive index changes attainable in liquid crystals are extraordinarily large, the efficiency of spectral tuning in the nematic phase may be reduced substantially due to strong surface anchoring of LC molecules. The latter, in fact, presents a serious problem for nanostructured LC-loaded metasurfaces operating in the visible and near-IR, and so far has made controlling the wavelength of their optical response practically impossible.^[21–23]

In this paper, we introduce a design of a near-IR active metasurface functionalized with a nematic LC, which allowed us to overcome the problem of strong anchoring and engage for the first time the mechanism of electrically controlled nanoscale in-plane switching of the LC director. As a result, the resonant response of the demonstrated metamaterial hybrid could be controlled both in terms of its magnitude and wavelength with the spectral tunability approaching the theoretical limit of 9%.

Dr. O. Buchnev, Dr. N. Podoliak, Prof. N. I. Zheludev, Dr. V. A. Fedotov
Optoelectronics Research Centre
University of Southampton
Southampton SO17 1BJ, UK
E-mail: O.Buchnev@soton.ac.uk;
vaf@orc.soton.ac.uk



Dr. O. Buchnev, Prof. N. I. Zheludev, Dr. V. A. Fedotov
EPSRC Centre for Photonic Metamaterials
University of Southampton
Southampton SO17 1BJ, UK

Prof. M. Kaczmarek
School of Physics and Astronomy
University of Southampton
Southampton SO17 1BJ, UK

Prof. N. I. Zheludev
Centre for Disruptive Photonic Technologies
Nanyang Technological University
Singapore 637371, Singapore

The copyright line for this article was changed on 22 January 2015 after original online publication.

This is an open access article under the terms of the Creative Commons Attribution License, which permits use, distribution and reproduction in any medium, provided the original work is properly cited.

DOI: 10.1002/adom.201400494

2. Active Metamaterial–LC Hybrid: Design and Fabrication

Although the in-plane LC switching has been experimentally demonstrated on the microscale for applications in LC

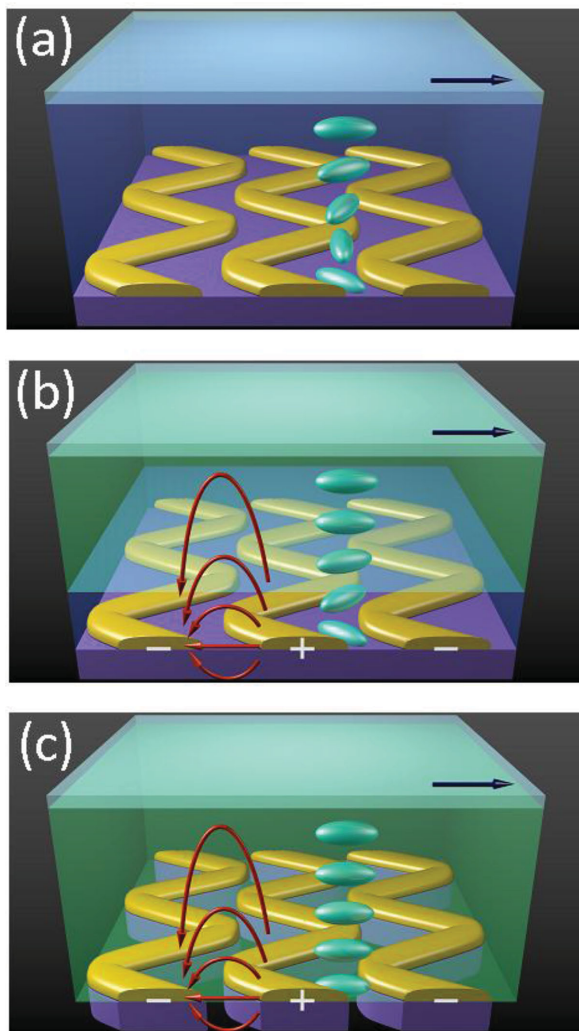


Figure 1. Schematic impression of a hybrid liquid-crystal cell with nanostructured metasurface electrically controlled via in-plane potentials. a) OFF state of the cell featuring initially twisted ordering in the bulk of the liquid crystal. b) ON state of the cell: LC ordering has been switched to planar (green) except for a very thin layer at the bottom (blue) with residual twist due to strong surface anchoring. c) ON state of the cell with suspended metasurface: switching from twisted to planar state is complete both in the bulk and in the plane of the metasurface. Black arrow indicates the direction of rubbing that sets LC alignment at the top cover.

displays^[24–26] and, recently in terahertz metamaterial-based modulators,^[27] its practical realization on the nanoscale is not straightforward due to strong surface anchoring. The problem of anchoring in nanostructured metamaterial–LC hybrids is illustrated in **Figure 1**. It has been recently shown that upon hybridization, the orientation of LC molecules near a metasurface is imposed by the pattern of its framework, rendering the nanostructure as an efficient alignment layer.^[28] Furthermore, the bonding of LC molecules to a metasurface appears to be robust enough to overcome the strong elastic forces characteristic of the nematic phase, and has been reported to sustain twisted ordering in the bulk of a liquid crystal when engaged in the conventional LC-cell configuration (see **Figure 1a**).^[22,28] The combination of elastic intermolecular coupling and robust surface

alignment makes a few tens of nanometers of the liquid crystal adjacent to the surface inactive,^[12,19,23,29,30] and this is what limits the tuneability of the nanostructured hybrid. Indeed, controlling the wavelength of its resonant response would require switching the LC director in the region of the strongest plasmonic fields, i.e., in the plane of the nanostructure and immediately above it, which is exactly where LC molecules could not be reoriented even with locally applied control fields (see **Figure 1b**).

We found that by reducing the contribution of the supporting substrate to the metamaterial surface area it became possible to minimize the anchoring forces in the resulting hybrid and engage in-plane switching of the LC director on the nanoscale (see **Figure 1c**). Combined with the usual volume switching, this enabled the realization of the full potential of the liquid crystal as a functional component of active metamaterial systems operating at optical frequencies.

The design of our metasurface was based on a double-periodic array of connected V-shaped plasmonic resonators forming a continuous “zig-zag”-wire pattern.^[28] It was fabricated by milling, with a focused ion-beam, an 80 nm thick gold film, which had been sputtered beforehand on a 100 nm thick silicon nitride (SiN) membrane, acting as the substrate. The milling also completely removed parts of the membrane, namely in the gaps between the zig-zag wires, thus yielding a gold metasurface fully suspended on SiN bridges (see **Figure 2a**). The elementary unit cell of the metamaterial array was rectangular with the size of $390 \times 580 \text{ nm}^2$. The wires had the width of approximately 220 nm, which rendered the pattern of the fabricated nanostructure as self-complementary (see **Figure 2b**). The zig-zag “packing” of the nanowires enabled to achieve a localized plasmonic resonance at the wavelength larger than the period of the pattern, which rendered the metasurface nondiffracting—a “medium of zero dimension” in the direction of light propagation. The overall size of the array was $16 \times 14 \mu\text{m}^2$ corresponding to approximately 10^3 unit cells. The odd and even nanowires were left connected to the opposite sections of the remaining gold film, which had been split to act as macroscopic voltage terminals (as shown in **Figure 2a**). This allowed us to apply an electric field in the plane of the metasurface, exploiting its framework as nanoscopic control electrodes. We also fabricated a reference structure, where the gold metasurface was supported by a complete 100 nm thick SiN membrane and featured the same design and dimensions as the suspended metasurface.

The response of the metamaterial structures was characterized in transmission at normal incidence in the 800–2000 nm range of wavelengths using linearly polarized light. **Figure 3a,b** present the results of our measurements for two orthogonal polarizations that corresponded to the plane of polarization being parallel (*x*-polarization) and perpendicular (*y*-polarization) to the length of the zig-zag nanowires. The spectra of both metasurfaces feature resonant bands centered at around $1.2 \mu\text{m}$, which appeared as either transmission pass- or stopband depending on the incident polarization. This remarkable property is characteristic of any self-complementary anisotropic pattern and follows directly from the Babinet principle.^[31] The observed resonances resulted from the excitation of standing plasmon waves in the straight segments of the zig-zag pattern and occurred when the plasmon wavelength became equal to twice the length of the individual segments.^[28] The slight differences in the spectra

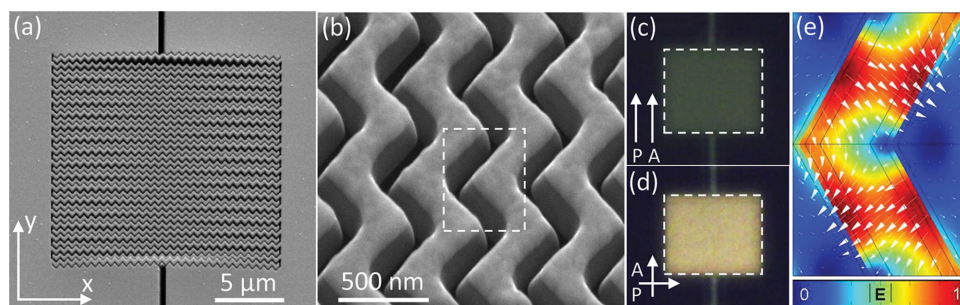


Figure 2. Suspended zig-zag metasurface. a) SEM image of the fabricated sample. b) SEM image of a small fragment of the metasurface taken at 52° to the structure's normal. Dashed box indicates elementary unit cell of zig-zag pattern. c,d) Images of LC-loaded metasurface in a twisted cell configuration made under a polarization optical microscope in transmission. Arrows indicate mutual orientations of the microscope's polarizer **P** and analyzer **A**. Dashed boxes indicate the area of the cell occupied by the metasurface. e) Distribution of the amplitude of induced electric field calculated in the plane of bare metasurface at the resonant wavelength of $1.2 \mu\text{m}$. White arrows show instantaneous direction of induced electric field.

of the suspended and reference metasurfaces are attributed to fabrication tolerances. Given the complimentary nature of the structures' transmission anisotropy, we will illustrate LC-enabled electrical tuning of the metamaterial response for *x*-polarized illumination only. Importantly, in this case the mode of excitation corresponds to the gap plasmon with its local electrical field oriented orthogonal to the nanowires, which was confirmed by our simulation results (see Figure 2e).

Each metasurface was functionalized with a nematic LC using the hybrid-twisted cell configuration, schematically shown in Figure 1a. A $2 \mu\text{m}$ thick layer of the LC mixture E7 (Merck) was sandwiched between the metasurface and a glass slide coated with a thin film of uniformly rubbed polyimide. The latter served to align the LC molecules in the direction of

rubbing at the top of the hybrid cell. The metasurface acted as an alignment layer at the bottom of the cell imposing the orientation of LC molecules parallel to gold nanowires, as was previously found in refs.[28,32] and confirmed by our observations of the resonance shift below. The zig-zag pattern was oriented orthogonal to the direction of rubbing of the cover glass, which introduced a twist in the elastic ordering of the LC layer.^[28] The advantage of the twisted cell configuration was twofold: i) the induced LC ordering suppressed the formation of domains and microscopic LC defects (which would reduce the transparency of the hybrid due to parasitic light scattering), and ii) the elastic deformation associated with the twisted nematic state naturally reduced the torque required for switching the LC molecules in the plane of the metasurface.

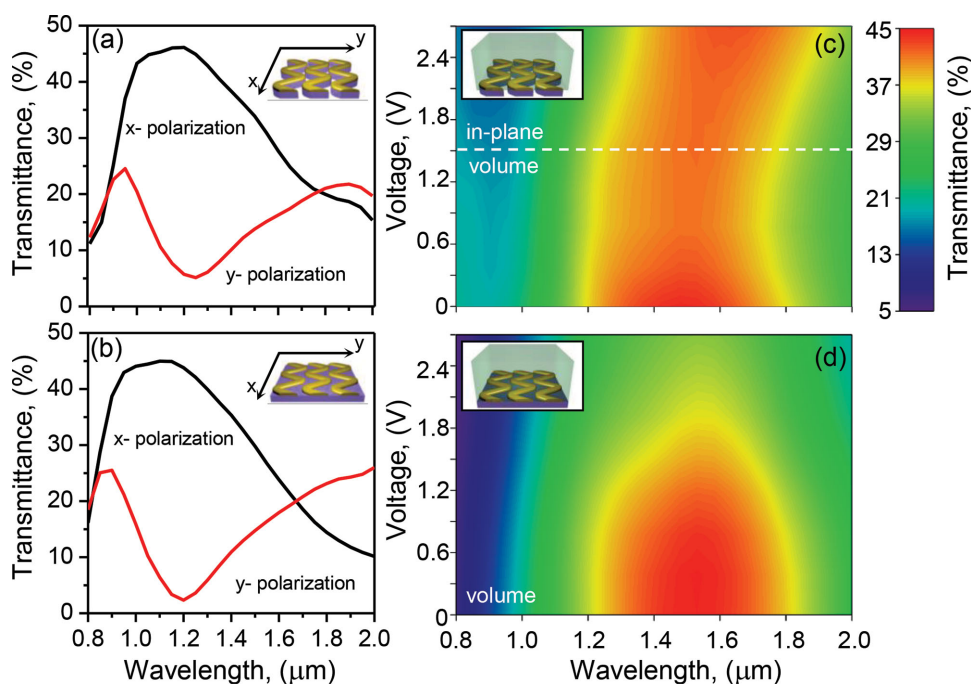


Figure 3. Electrically tunable near-IR response of zig-zag metasurfaces. a,b) Transmission spectra of correspondingly suspended and reference bare metasurfaces measured for *x*- and *y*-polarization. c,d) Transmittance of hybrid LC cells with correspondingly suspended and reference metasurfaces measured for *x*-polarization as a function of wavelength and potential difference applied between zig-zag nanowires. Dashed line indicates the transition between two regimes of electrical tuning corresponding to volume and in-plane switching of the hybrid cell.

The high quality of the assembled hybrid cells was visually confirmed in transmission using a polarization optical microscope (see Figure 2c,d). The cells appeared as uniform defect-free rectangular patches that changed their brightness in a wide range depending on the mutual orientation of the polarizer and analyzer. The dark state was observed when the polarizer and analyzer were aligned (Figure 2c), while the bright state—when the two were crossed (Figure 2d). The residual transmittance in Figure 2c was the result of a slight misalignment between the direction of rubbing of the cover glass and the zig-zag pattern. This misalignment, however, could not significantly impact the in-plane switching, as its mechanism does not rely on achieving the perfect (90°) twist in the bulk of the nematic.

3. Results and Discussion

Figure 3c,d show transmission spectra of LC-loaded metasurfaces that were measured for a potential difference in the range from 0 to 2.7 V applied across the gaps of the zig-zag pattern. To avoid the accumulation of an electric charge and, correspondingly, the appearance of a double-charged layer at the interface between the liquid crystal and electrodes we employed a common driving scheme, where the sign of the control voltage is alternated with the frequency of 1 kHz. The samples were illuminated from their bottom side so that light propagated through the metamaterial structure first before entering LC layer. This ensured that any changes of the polarization state of light induced by the *bulk* of the liquid crystal had no effect on the excitation of the metasurfaces. Furthermore, since the detector was polarization insensitive, changes in the LC birefringence could not contribute to the modifications of the spectra described below. At 0 V the transmission passband of both samples appeared redshifted by about 300 nm (≈24%) with respect to that of the bare metasurfaces. The direction of the shift was consistent with an increase of the average refractive index in the vicinity of the gold nanowires due to the addition of the liquid crystal. The magnitude of the shift corroborates the observation made earlier that the LC molecules tend to align parallel to the nanowires. Indeed, if we assume the local refractive index of E7 (which replaces air) to be ordinary $n_o = 1.50$,^[33] and given that the refractive index of the substrate $n_{\text{SiN}} = 1.98$ ^[34] the corresponding increase of the average index is estimated to be 25%.

The application of an electrical field was seen to further change the transmission spectra of both metasurfaces, but the changes followed different trends. In the case of the suspended nanostructure two distinct stages of tuning could be identified (see Figure 3c and Figure S1a, Supporting Information). The first stage corresponded to a gradual decrease of the transmittance with increasing voltage in the range from 0 to about 1.5 V. When the voltage exceeded 1.5 V the resonance started to shift towards longer wavelengths, which signified the onset of the second stage—spectral tuning. At 2.7 V the magnitude of the spectral shift was seen to reach ≈110 nm (7%). In the case of the reference metasurface we observed only a gradual decrease of its transmittance (see Figure 3d and Figure S1b, Supporting Information).

Clearly, electrically controlled redshift must have resulted from a further increase of the effective dielectric constant near

the suspended gold nanowires, which could happen only if the applied field had reoriented some of the LC molecules in the plane of the metasurface. Assuming that the refractive index of E7 switched from ordinary, n_o , to extraordinary, $n_e = 1.70$,^[33] everywhere around the nanowires (including the gaps), we estimated the upper limit for the average refractive index change to be 9%. The estimate is in very good agreement with the value of the observed shift, which suggests that the suspended design had enabled almost complete in-plane switching of the liquid crystal. The decrease of the transmittance observed in both cases is attributed to the bulk LC switching, when stray electric fields produced by in-plane electrode configuration alter elastic ordering of LC molecules in the volume of the twisted cell (see illustrations in Figure 1). The ordering begins to untwist near the surface of the glass cover, since here the LC director is nearly parallel to the horizontal component of the field and therefore is easier to reorient. With increasing voltage, the stray fields affect deeper layers of the cell where elastic forces are stronger, and the induced new (planar) LC state gradually propagates towards the metasurface. It should be mentioned that the absence of in-plane switching in the reference case cannot be attributed to the stray surface conductance of the SiN membrane or short circuits that might potentially weaken the applied electric field. The latter would result in local heating of the liquid crystal and lead to disturbances easily detectable under the microscope. Furthermore, lowering the in-gap voltage would also reduce the strength of stray electric fields and hence lessen the effect of the bulk switching.

The microscopic nature of the switching mechanisms was confirmed numerically by simulating electrically induced LC elastic distortions for the hybrid-cell configuration. Given that the reorientation of LC molecules happened on the scale much smaller than the size of the metamaterial unit cell, the metasurfaces could be modeled as periodic grids of straight nanowires. This allowed us to reduce the complexity of the problem and perform rigorous simulations in just two dimensions. With periodic boundary conditions applied to their sidewalls, the simulated domains accurately represented the cross sections of the fabricated cells, both in terms of their geometry and dimensions (see Figure 4a). The width of each domain was set to two periods of the corresponding metasurface, which accounted for the periodicity of the spatially alternating potential applied to the nanowires.

The LC-director field \mathbf{n} was characterized by two angles, θ and ϕ . The former (polar angle) described the local orientation of the director in the plane of the cross section (yz -plane), while the latter (azimuthal angle)—in the plane parallel to the metasurface, i.e., xy -plane. The spatial dependences of $\theta(y,z)$ and $\phi(y,z)$ were obtained by minimizing numerically the LC free-energy functional:

$$F = \int_V \left\{ \frac{K_1}{2} (\nabla \cdot \mathbf{n})^2 + \frac{K_2}{2} (\mathbf{n} \cdot [\nabla \times \mathbf{n}])^2 + \frac{K_3}{2} (\mathbf{n} \times [\nabla \times \mathbf{n}])^2 - \frac{1}{2} \epsilon_0 \Delta \epsilon (E \cdot \mathbf{n})^2 \right\} dV \quad (1)$$

where $K_{1,2,3}$ are the elastic constants of the liquid crystal and $\Delta \epsilon$ is its DC dielectric anisotropy.^[4]

Supported by the experimental findings,^[28,32] our model assumed strong anchoring of LC molecules at the surfaces

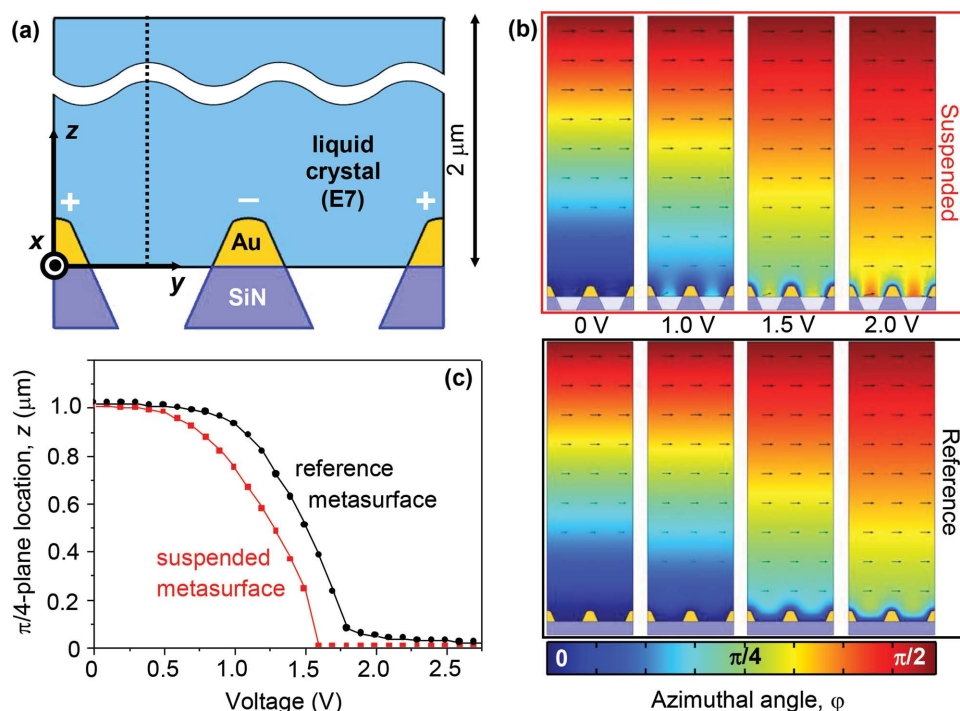


Figure 4. Electrically induced elastic distortions of liquid crystal in hybrid twisted cells. a) Schematic of the simulation domain representing a two-period wide cross section of the hybrid cell with suspended metasurface. b) Spatially dependent orientation of LC director above suspended and reference metasurfaces calculated for 0, 1.0, 1.5, and 2.0 V of the potential difference applied between their nanowires. Color maps show spatial variations of the director's azimuthal angle ϕ , where $\phi = 0$ and $\phi = \pi/2$ correspond to the director being orthogonal and parallel to the plane, respectively. Arrows represent local projections of the director onto the plane of the plot. c) Location of the effective interface between planar and twisted LC (the $\phi = \pi/4$ plane) as a function of applied voltage. Propagation of the interface was evaluated along the vertical cross-section indicated in panel (a) by the dashed line.

of the nanowires and membrane with local orientation of the director corresponding to $\phi = 0$ (parallel to the nanowires). In the case of the suspended metasurface the gaps were assumed to be partially infiltrated by the liquid crystal, which had formed *free* flat surfaces terminating at the border between the SiN bridges and nanowires (see Figure 4a). This assumption was verified by a close inspection of the sample under a polarization microscope, which revealed no traces of the liquid crystal on silicon-nitride side of the metasurface. Furthermore, additional simulations showed that the complete infiltration could not significantly affect the in-plane reorientation of LC molecules, leading only to a slight delay of the bulk switching onset in terms of the bias voltage (see Figure S2, Supporting Information). To further simplify our model, the effect of the alignment layers at the top of the cells was introduced through the strong-anchoring boundary condition with the orientation of the LC director corresponding to $\phi = \pi/2$ (orthogonal to the nanowires).

The free-energy functional (Equation 1) was minimized using FEM-based solver implemented in COMSOL Multiphysics. The software was also used for calculating the spatial distribution of the control electric field, which had been coupled with the functional through a LC-dielectric tensor. The results of our simulations are presented in Figure 4b. At 0 V the entire bulk of the hybrids cells appears in the twisted state, which may be seen as a gradual variation of colors from red ($\phi = \pi/2$) to blue ($\phi = 0$), or as a change of the in-plane component of \mathbf{n} (shown as arrows) across the height of the simulated domains.

With increasing voltage the red-shaded region corresponding to the LC planar state (arrows of maximal length) progressively expands towards the bottom of the cells and at 2 V completely replaces the twisted state above the suspended metasurface.

The evolution of the LC ordering in both cells is further illustrated in Figure 4c in terms of the propagation of an effective interface between planar and twist regions defined by the $\phi = \pi/4$ plane. Clearly, in the case of the suspended metasurface the changes are always seen at lower voltage. The transition between the volume and in-plane LC-switching regimes takes place when the interface reaches the bottom of the cell. For the suspended metasurface this happens at around 1.5 V, which agrees well with the experimental observation. In the reference case, however, the interface does not seem to reach the metasurface below 2.7 V, so that a thin layer of the twisted LC is always present above the nanostructure.

4. Conclusions

In conclusion, we proposed and realized a design for an active near-IR metasurface, functionalized with a layer of nematic LC, which for the first time fully engaged the mechanism of electrically controlled nanoscale in-plane switching of LC director. Our design exploited the combination of suspended plasmonic resonators and twisted LC, which enabled us to minimize the detrimental effect of strong surface anchoring of LC molecules. As the result, the resonant response of the fabricated

metamaterial hybrid could be controlled both in terms of its magnitude and wavelength. In particular, the spectral tuning was experimentally observed for the different levels of applied voltage in the range 1.5–2.7 V, where it reached 110 nm ($\approx 7\%$). The microscopic nature of the two-way control mechanism was confirmed numerically by simulating reorientation of LC director in the hybrid structure in the presence of an applied DC electric field. The approach demonstrated here thus allowed us to utilize the full potential of liquid crystals as the functional component of active metamaterial systems operating at optical frequencies, which paves a way towards the development of compact multifunctional metamaterial-based photonic modulators and switches. The range of potential applications of the demonstrated concept might be readily expanded by introducing an asymmetry or structural gradient into the fabric of the zig-zag metasurface, which will turn it into a tunable ultrathin polarization control element, or enable active control of optical wavefronts and beam steering. We also anticipate that by engaging LC switching at the nanoscale one may achieve a faster response compared to that of the common bulk LC-switching schemes.

Supporting Information

Supporting Information is available from the Wiley Online Library or from the author.

Acknowledgements

This work is supported by the UK's Engineering and Physical Sciences Research Council through Career Acceleration Fellowship EP/G00515X/1 (V.A.F.), Programme grant EP/G060363/1 and grant EP/J012874/1, by the Royal Society, and by the MOE Singapore grant MOE2011-T3-1-005.

Received: October 27, 2014

Revised: November 23, 2014

Published online: January 2, 2015

- [1] E. Plum, V. A. Fedotov, A. S. Schwanecke, N. I. Zheludev, Y. Chen, *Appl. Phys. Lett.* **2007**, *90*, 223113.
- [2] F. M. Huang, T. S. Kao, V. A. Fedotov, Y. Chen, N. I. Zheludev *Nano Lett.* **2008**, *8*, 2469.
- [3] F. Aieta, P. Genevet, M. A. Kats, N. Yu, R. Blanchard, Z. Gaburro, F. Capasso, *Nano Lett.* **2012**, *12*, 4932.
- [4] S. Ishii, V. M. Shalaev, A. V. Kildishev, *Nano Lett.* **2013**, *13*, 159.
- [5] T. Roy, E. T. F. Rogers, N. I. Zheludev, *Opt. Express* **2013**, *21*, 7577.
- [6] A. S. Schwanecke, V. A. Fedotov, V. V. Khardikov, S. L. Prosvirnin, Y. Chen, N. I. Zheludev, *Nano Lett.* **2008**, *8*, 2940.
- [7] E. Plum, X.-X. Liu, V. A. Fedotov, Y. Chen, D. P. Tsai, N. I. Zheludev, *Phys. Rev. Lett.* **2009**, *102*, 113902.
- [8] N. Yu, P. Genevet, M. A. Kats, F. Aieta, J.-F. Tetienne, F. Capasso, Z. Gaburro, *Science* **2011**, *334*, 333.
- [9] A. V. Kildishev, A. Boltasseva, V. M. Shalaev, *Science* **2013**, *339*, 6125.
- [10] N. I. Zheludev, *Science* **2010**, *328*, 582.
- [11] N. I. Zheludev, Y. S. Kivshar, *Nat. Mater.* **2012**, *11*, 917.
- [12] P. G. de Gennes, J. Prost, *The Physics of Liquid Crystals*, Clarendon Press, Oxford, UK **1993**.
- [13] F. Zhang, Q. Zhao, L. Kang, D. P. Gaillot, X. Zhao, J. Zhou, D. Lippens, *Appl. Phys. Lett.* **2008**, *92*, 193104.
- [14] Q. Zhao, L. Kang, B. Du, B. Li, J. Zhou, H. Tang, Z. Liang, B. Zhang, *Appl. Phys. Lett.* **2007**, *90*, 011112.
- [15] F. Zhang, W. Zhang, Q. Zhao, J. Sun, K. Qiu, J. Zhou, D. Lippens, *Opt. Express* **2011**, *19*, 1563.
- [16] Sh. Xiao, U. K. Chettiar, A. V. Kildishev, V. Drachev, I. C. Khoo, V. M. Shalaev, *Appl. Phys. Lett.* **2009**, *95*, 033115.
- [17] B. Kang, J. H. Woo, E. Choi, H. H. Lee, E. S. Kim, J. Kim, T.-J. Hwang, Y.-S. Park, D. H. Kim, J. W. Wu, *Opt. Express* **2010**, *18*, 16492.
- [18] Y. J. Liu, G. Y. Si, E. S. P. Leong, N. Xiang, A. J. Danner, J. H. Teng, *Adv. Mater.* **2012**, *24*, 131.
- [19] A. Minovich, J. Farnell, D. N. Neshev, I. McKerracher, F. Karouta, J. Tian, D. A. Powell, I. V. Shadrivov, H. H. Tan, C. Jagadish, Yu. S. Kivshar, *Appl. Phys. Lett.* **2012**, *100*, 121113.
- [20] P. R. Evans, G. A. Wurtz, W. R. Hendren, R. Atkinson, W. Dickson, A. V. Zayats, R. Pollard, *Appl. Phys. Lett.* **2007**, *91*, 043101.
- [21] P. A. Kossyrev, A. J. Yin, S. G. Cloutier, D. A. Cardimona, D. H. Huang, P. M. Alsing, J. M. Xu, *Nano Lett.* **2005**, *5*, 1978.
- [22] M. Decker, Ch. Kremers, A. Minovich, I. Staude, A. E. Miroshnichenko, D. Chigrin, D. N. Neshev, Ch. Jagadish, Yu. S. Kivshar, *Opt. Express* **2013**, *21*, 8879.
- [23] I. C. Khoo, *Prog. Quantum Electron.* **2014**, *38*, 77.
- [24] M. Oh-e, K. Kondo, *Appl. Phys. Lett.* **1995**, *67*, 3895.
- [25] M. Oh-e, K. Kondo, *Appl. Phys. Lett.* **1996**, *69*, 623.
- [26] S. H. Lee, S. L. Lee, H. Y. Kim, *Appl. Phys. Lett.* **1998**, *73*, 2881.
- [27] O. Buchnev, J. Wallauer, M. Walther, M. Kaczmarek, N. I. Zheludev, V. A. Fedotov, *Appl. Phys. Lett.* **2013**, *103*, 141904.
- [28] O. Buchnev, J. Y. Ou, M. Kaczmarek, N. I. Zheludev, V. A. Fedotov, *Opt. Express* **2013**, *21*, 1633.
- [29] M. Decker, A. Minovich, Ch. Kremers, A. Miroshnichenko, H. H. Tan, D. Chigrin, D. Neshev, Ch. Jagadish, Yu. Kivshar, presented at *Proc. Metamaterials 2012*, St. Petersburg, Russia **2012**.
- [30] Sh. T. Wu, U. Efron, *Appl. Phys. Lett.* **1986**, *48*, 624.
- [31] F. Falcone, T. Lopetegui, M. A. G. Laso, J. D. Baena, J. Bonache, M. Beruete, R. Marqués, F. Martín, M. Sorolla, *Phys. Rev. Lett.* **2004**, *93*, 197401.
- [32] P. N. Sanda, D. B. Dove, H. L. Ong, S. A. Jansen, R. Hoffmann, *Phys Rev A* **1989**, *39*, 2653.
- [33] J. Li, Sh. T. Wu, S. Brugioni, R. Meucci, S. Faetti, *J. Appl. Phys.* **2005**, *97*, 073501.
- [34] T. Bååk, *Appl. Opt.* **1982**, *21*, 1069.